

Statistical Physics of Traffic Flow¹

Andreas Schadschneider^{a,2}

^a*Institut für Theoretische Physik, Universität zu Köln, D-50923 Köln, Germany*

Physica **A285**, 101 (2000)

Abstract

The modelling of traffic flow using methods and models from physics has a long history. In recent years especially cellular automata models have allowed for large-scale simulations of large traffic networks faster than real time. On the other hand, these systems are interesting for physicists since they allow to observe genuine nonequilibrium effects. Here the current status of cellular automata models for traffic flow is reviewed with special emphasis on nonequilibrium effects (e.g. phase transitions) induced by on- and off-ramps.

Key words: Cellular automata, complex systems, nonequilibrium physics

1 Introduction

Despite the long history of application of methods from physics to traffic flow problems (going back to the fifties) it has only recently blossomed into a successful field of “exotic statistical physics” [1]. Until a few years ago most approaches were based on “classical” methods from physics, especially from mechanics and hydrodynamics. In general one can distinguish *microscopic* and *macroscopic* approaches.

In *microscopic models* individual vehicles are distinguished. A typical example are the so-called *car-following theories* [2,3]. For each car one writes an

¹ Supported by SFB 341 (Köln-Aachen-Jülich)

² E-mail: as@thp.uni-koeln.de

equation of motion which is the analogue of Newton's equation. The basic philosophy of the car-following approach can be summarized by the equation $[Response]_n = \kappa_n [Stimulus]_n$ for the n -th vehicle. Each driver n responds to the surrounding traffic conditions which constitute the stimulus for his reaction. The constant of proportionality κ_n is also called sensitivity. Usually also the reaction-time of the drivers is taken into account. A typical example is the *follow-the-leader* model [3] where the stimulus is given by the velocity difference to the next car ahead. Assuming that drivers tend to move at the same speed as the leading car the equations of motion are given by $\ddot{x}_n(t) = \kappa_n [\dot{x}_{n+1}(t) - \dot{x}_n(t)]$. In order to obtain realistic behaviour the sensitivity κ_n has to become a function of the velocity and the distance between the cars, $\kappa_n = \kappa_n(v_n, x_{n+1} - x_n)$. In recent years the so-called *optimal-velocity model* [4] has successfully been used. Here the acceleration is determined by the difference of the actual velocity $v_n(t)$ and an optimal velocity $V^{opt}(\Delta x_n)$ which depends on the distance Δx_n to the next car. The equations of motion are then of the form $\ddot{x}_n(t) = \kappa_n [V^{opt}(\Delta x_n) - v_n(t)]$.

In *macroscopic models* one does not distinguish individual cars. Instead a "coarse-grained" fluid-dynamical description in terms of densities $c(x, t)$ and flows $J(x, t)$ is used. Traffic is then viewed as a compressible fluid formed by the vehicles. Density and flow are related through a continuity equation which for closed systems takes the form $\partial c / \partial t + \partial J / \partial x = 0$. Since this is only one equation for two unknown functions one needs additional information. In one of the first traffic models Lighthill and Whitham [5] assumed that $J(x, t)$ is determined by $c(x, t)$, i.e. $J(x, t) = J(c(x, t))$. Inserting this assumption into the continuity equation yields the so-called Lighthill-Whitham equation $\partial c / \partial t + v_g \partial c / \partial x = 0$ with $v_g = dJ/dc$. However, for a more realistic description of an traffic additional equation, the analogue of the Navier-Stokes equation for fluids, describing the time-dependence of the velocities $v_n(x, t)$ has to be considered instead of the simple Lighthill-Whitham assumption.

The first approach borrowing ideas from statistical physics is the *kinetic theory of vehicular traffic* [6]. Here traffic is treated as a gas of interacting particles. The interactions are described by a dynamical equation in phase space which is the analogue of the Boltzmann equation in the kinetic theory of gases.

This is only a a very brief overview over the different approaches for the description of traffic flow. For a more complete exposition of the models and their merits we refer to the literature, e.g. [1,6–13]. Nice overviews over the physics of related nonequilibrium models can be found in [14–17]. In the following we concentrate on a class of models developed in the last few years, namely (probabilistic) cellular automata. These models describe stochastic processes and are therefore of general interest for statistical physics [18,19]. An extensive review of the application of cellular automata to traffic flow and related systems can be found in [1]. Here we focus on aspects that have not been

discussed in much detail in [1], e.g. the effects of on- and off-ramps.

2 Some empirical facts

The most simple empirical facts that should be reproduced by any traffic model are the spontaneous formation of jams and the characteristic form of the flow-density relation, the so-called fundamental diagram. The space-time plot of Fig. 1 shows the formation and propagation of a traffic jam. In the beginning, the vehicles are well separated from each other. Then, without any obvious reason like an accident or road construction, a dense region appears due to fluctuations. This finally leads to the formation of a jam which remains stable for a certain period of time but disappears again without any obvious reason. During its lifetime the front of the jam moves backwards against the driving direction of the cars with a characteristic velocity of approximately 15 km/h.

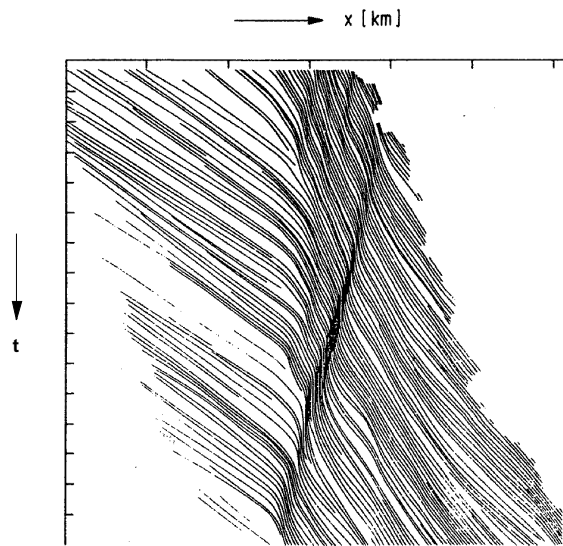


Fig. 1. Trajectories of individual vehicles on a single lane of a multi-lane highway showing the spontaneous formation of a jam (from [20]).

A more detailed analysis of traffic jams in absence of hindrances has been given by Kerner and Rehborn [21–23]. They found that the upstream velocity and, therefore, the outflow from a jam is approximately constant. The outflow from a jam and the velocity of the jam fronts are now regarded as two important empirical parameters of highway traffic which can be used for calibrating theoretical models.

Fig. 2 shows a typical fundamental diagram obtained from empirical data. One

can clearly distinguish two regions, the free-flow regime at small densities and the congested regime at high densities. In the free-flow regime the cars do not hinder each others motion and therefore the flow grows linearly with density. In the congested regime however, the motion of the vehicles is dominated by the hindrance due to other cars. Here the flow decreases with increasing density.

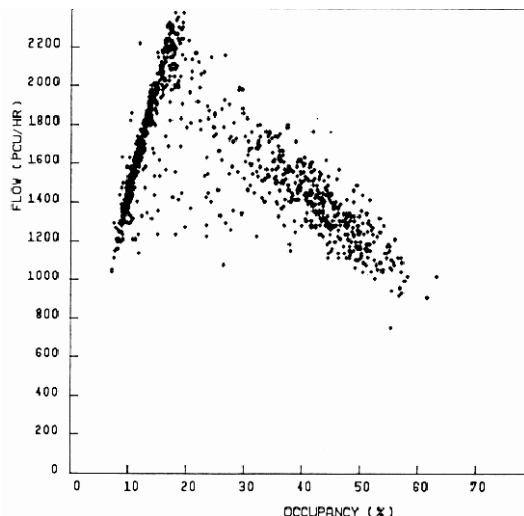


Fig. 2. Empirical data for flow and density (occupancy) measured directly by counting loops on a Canadian highway. Each point in the diagram corresponds to an average over a time interval of five minutes (from [24]).

These considerations only give the basic structure of the fundamental diagram. In Sec. 4 a more detailed analysis of empirical data will be presented which reveals a much richer structure, e.g. the existence of hysteresis and metastable states. Furthermore in the congested regime one can distinguish two different phases, namely stop-and-go traffic and synchronized flow.

3 Cellular automata models

The Nagel-Schreckenberg (NaSch) model [25] is a probabilistic cellular automaton (CA) able to reproduce the basic features of traffic flow as discussed in Sec. 2. In a CA not only space and time are discrete, but also the state variable. In the NaSch model, each cell can be empty or occupied by exactly one car (Fig. 3). The state of the car is then characterized by its velocity v which can take one of the $v_{max} + 1$ allowed *integer* values $v = 0, 1, \dots, v_{max}$. Suppose, x_n and v_n denote the position and velocity, respectively, of the n -th vehicle. Then, $d_n = x_{n+1} - x_n$, is the gap in between the n -th car and the car in front of it at time t . At each time step $t \rightarrow t + 1$, the arrangement of the N cars on a finite lattice of length L (i.e. for a global density $\rho = N/L$) is updated *in parallel* according to the following "rules":

Step 1: Acceleration.

If $v_n < v_{max}$, the speed of the n -th car is increased by one, i.e.

$$v_n \rightarrow \min(v_n + 1, v_{max}) \quad (\text{U1}).$$

Step 2: Deceleration (due to other cars).

If $d_n \leq v_n$, the speed of the n -th car is reduced to $d_n - 1$, i.e.,

$$v_n \rightarrow \min(v_n, d_n - 1) \quad (\text{U2}).$$

Step 3: Randomization.

If $v_n > 0$, the speed of the n -th car is decreased randomly by unity with probability p , i.e.,

$$v_n \rightarrow \max(v_n - 1, 0) \quad \text{with probability } p \quad (\text{U3}).$$

Step 4: Vehicle movement.

Each car is moved forward according to its new velocity determined in Steps 1–3, i.e.

$$x_n \rightarrow x_n + v_n \quad (\text{U4}).$$

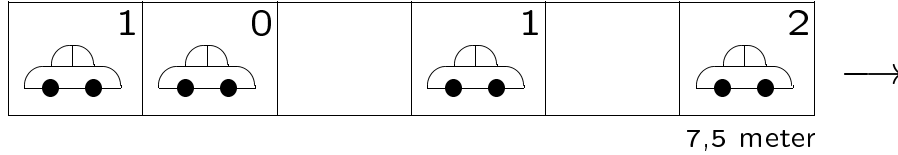


Fig. 3. A typical configuration in the NaSch model. The number in the upper right corner is the speed of the vehicle.

The NaSch model is a minimal model in the sense that all the four steps are necessary to reproduce the basic features of real traffic; however, additional rules are needed to capture more complex situations. Step 1 reflects the general tendency of the drivers to drive as fast as possible without crossing the maximum speed limit. Step 2 is intended to avoid collision between the cars. The randomization in step 3 takes into account the different behavioural patterns of the individual drivers, especially, nondeterministic acceleration as well as overreaction while slowing down; this is crucially important for the spontaneous formation of traffic jams. Even changing the precise order of the steps of the update rules stated above would change the properties of the model. E.g. after changing the order of steps 2 and 3 there will be no overreactions at braking and thus no spontaneous formation of jams (see below). The NaSch model may be regarded as stochastic CA [18]. In the special case $v_{max} = 1$ the deterministic limit of the NaSch model is equivalent to the CA rule 184 in Wolfram's notation [18].

The use of a *parallel* updating scheme (instead of a random-sequential one) is crucial [26] since it takes into account the reaction-time and can lead to a chain of overreactions. Suppose, a car slows down due the randomization step. If the density of cars is large enough this might force the following car also to brake in the deceleration step. In addition, if p is larger than zero, it might brake even further in Step 3. Eventually this can lead to the stopping of a car, thus creating a jam. This simple mechanism of spontaneous jam formation is rather realistic and cannot be modeled by the random-sequential update.

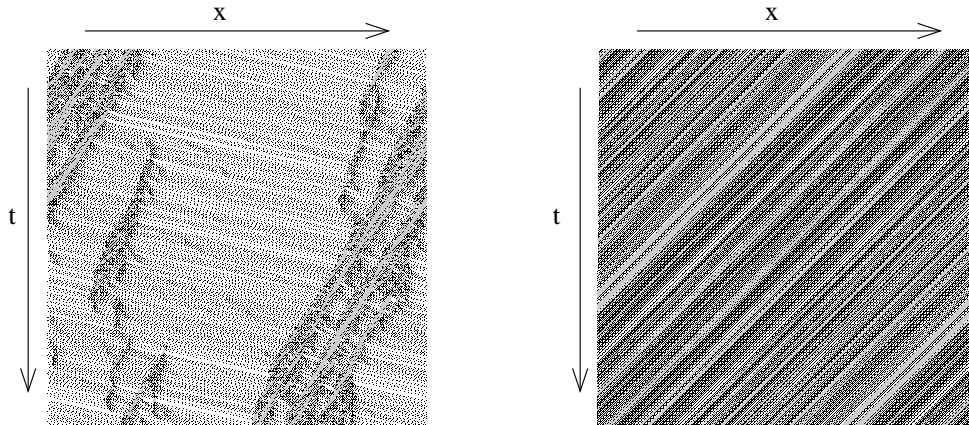


Fig. 4. Typical space-time diagrams of the NaSch model with $v_{max} = 5$ and (a) $p = 0.25, \rho = 0.20$, (b) $p = 0, \rho = 0.5$.

Space-time diagrams showing the time evolutions of the NaSch model demonstrate that no jam is present at sufficiently low densities, but spontaneous fluctuations give rise to traffic jams at higher densities (Fig. 4(a)). From Fig. 4(b) it should be obvious that the *intrinsic stochasticity* of the dynamics, arising from non-zero p , is essential for triggering the jams. For a realistic description of highway traffic [25], the typical length of each cell should be about 7.5 m which is the space occupied by a car in a dense jam. When $v_{max} = 5$ each time step corresponds to approximately 1 sec of real time which is of the order of the shortest relevant timescale in real traffic, namely the reaction time of the drivers.

3.1 Open boundary conditions

For $v_{max} = 1$ the NaSch model reduces to the totally asymmetric simple exclusion process (ASEP) with parallel update. The ASEP is the simplest prototype model of interacting systems driven far from equilibrium [14,17]. In the ASEP (Fig. 5) a particle can move forward one cell with probability³ p if

³ Note that conventionally the hopping rate in the ASEP is denoted as p . Since in the NaSch model p is the braking probability the hopping rate in the ASEP (for

the lattice site immediately in front of it is empty. In addition one considers open boundary conditions. If the first cell is empty a particle will be inserted there with probability α . If the last cell is occupied the particle will be removed with probability β .

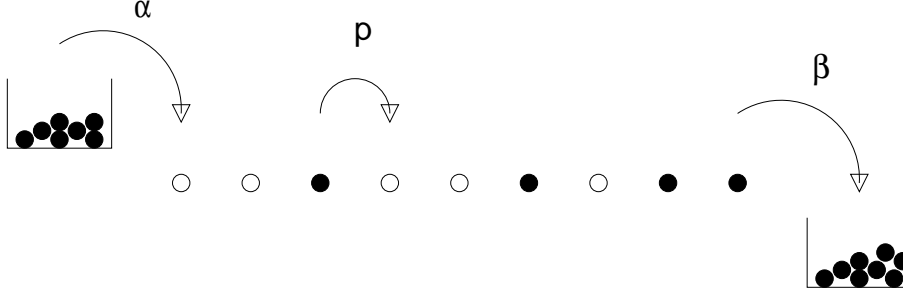


Fig. 5. The asymmetric simple exclusion process.

By varying the boundary rates α and β one obtains a surprisingly rich phase diagram (see Fig. 6) which is qualitatively the same for all types of dynamics [27–31]. Three phases can be distinguished by the functional dependence of the current through the system on the system parameters. In the low-density phase A ($\alpha < \beta, \alpha_c(p)$) the current is independent of β . Here the current is limited by the rate α which then dominates the behaviour of the system. In the high-density phase B ($\beta < \alpha, \beta_c(p)$) the behaviour is dominated by the output rate β and the current is independent of α . In the maximum current phase C ($\alpha > \alpha_c(p)$ and $\beta > \beta_c(p)$) the limiting factor for the current is the bulk rate $q = 1 - p$. Here the current becomes independent of both α and β .

The transitions between the phases can be characterized by the behaviour of two correlation lengths ξ_α and ξ_β which only depend on p and α or β . Apart from ξ_α and ξ_β also a third length $\xi^{-1} = |\xi_\alpha^{-1} - \xi_\beta^{-1}|$ plays an important role.

The transition from A (B) to C is continuous with diverging correlation length ξ_α (ξ_β). The transition from the high- to the low-density phase is of first order. Here both ξ_α and ξ_β are finite, but ξ diverges. On the transition line one finds a linear density profile created by the diffusion of a domain wall between a low-density region at the left end of the chain and a high-density region at the right end.

In [32] a nice physical picture has been developed which explains the structure of the phase diagram not only qualitatively, but also (at least partially) quantitatively. The phase diagram of the open system is completely determined by the fundamental diagram of the periodic system through an extremal-current principle [33] and therefore independent of the microscopic dynamics of the model.

$v_{max} = 1$) becomes $q = 1 - p$.

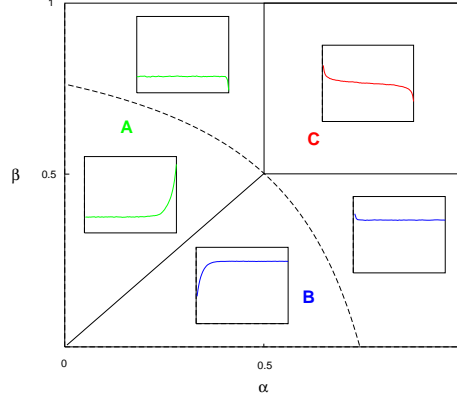


Fig. 6. Phase diagram of the ASEP. The inserts show the typical form of the density profiles.

Fig. 7 shows the full phase diagram of the NaSch model with open boundary conditions and $v_{max} = 4$. As predicted by the extremal-current principle the same phases as in the case $v_{max} = 1$ described above appear. Instead of using input- and output-rates at the boundaries here reservoirs have been introduced which induce effective densities ρ^- and ρ^+ near the boundaries. In order to allow for an easier comparison with empirical data obtained near ramps (see Sec. 5.2) the phases are denoted as "free-flow" and "congested" instead of "low-density" and "high-density".

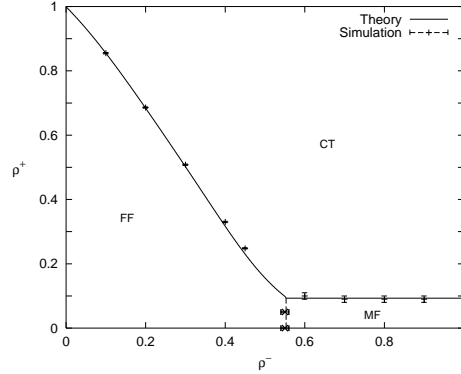


Fig. 7. Phase diagram of the NaSch model with open boundaries for $p = 0.25, v_{max} = 4$ coupled to reservoirs with densities $\bar{\rho}^-$ and $\bar{\rho}^+$ which induce the upstream-density ρ^- and the downstream-density ρ^+ . The phases are: free-flow (FF), congested traffic (CT), maximal flow (MF) phase.

4 Generalizations and extensions of the NaSch model

4.1 Metastability, hysteresis and slow-to-start rules

Measurements on real traffic have revealed that traffic flow can exhibit metastability and hysteresis effects [23]. Fig. 8(a) shows a schematic fundamental diagram with a metastable branch. In the density interval $\rho_1 < \rho < \rho_2$ the flow is not uniquely determined but depends on the history of the system. Here a metastable high-flow branch exists. Closely related is the observation of hysteresis effects. Fig 8(b) shows a clear hysteresis loop obtained from time-traced measurements of the flow [24].

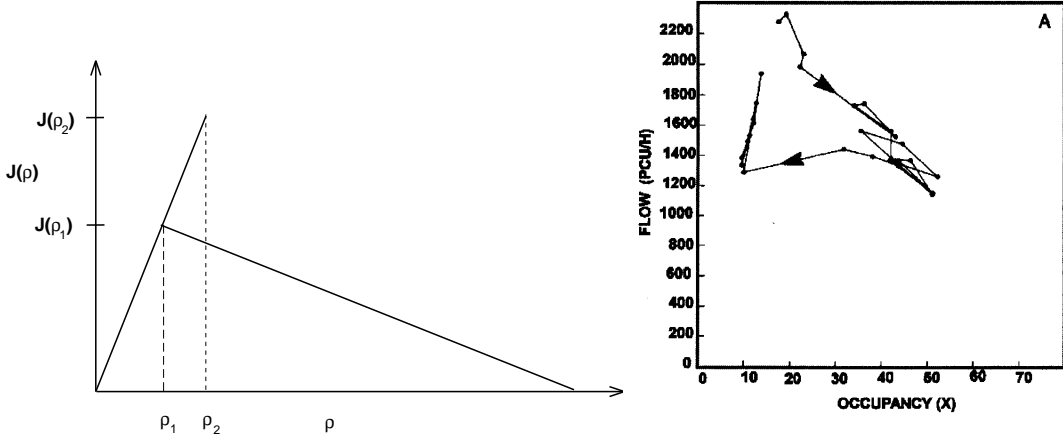


Fig. 8. (a) Schematic form of a fundamental diagram with metastable high-flow states, (b) Time-series of empirical flow data showing hysteresis.

The NaSch model in its simplest form as introduced in Sec. 3 does not exhibit metastable states and hysteresis. However, a simple generalization exists which is able to reproduce these effects. It is the so-called Velocity-Dependent-Randomization (VDR) model [34]. Here, in contrast to the original NaSch model, the randomization parameter depends on the velocity of the car, $p = p(v)$. The rules of Sec. 3 are supplemented by a new rule,

Step 0: Determination of the randomization parameter. The randomization parameter used in step 3 for the n -th car is given by $p = p(v_n(t))$.

This new step has to be carried out before the acceleration step 1. The randomization parameter used in step 3 depends on the velocity $v_n(t)$ of the n -th car after the previous timestep. Most relevant for an understanding of the occurrence of metastability and hysteresis are simple slow-to-start rules where one chooses [34]

$$p(v) = \begin{cases} p_0 & \text{for } v = 0, \\ p & \text{for } v > 0, \end{cases} \quad (1)$$

with $p_0 > p$. This means that cars which have been standing in the previous timestep have a higher probability p_0 of braking in the randomization step than moving cars.

Fig. 9 shows a typical fundamental diagram obtained from computer simulations of the VDR model. It can be clearly seen that it has the same form as Fig. 8(a). Over a certain density interval $J(\rho)$ can take one of the two val-

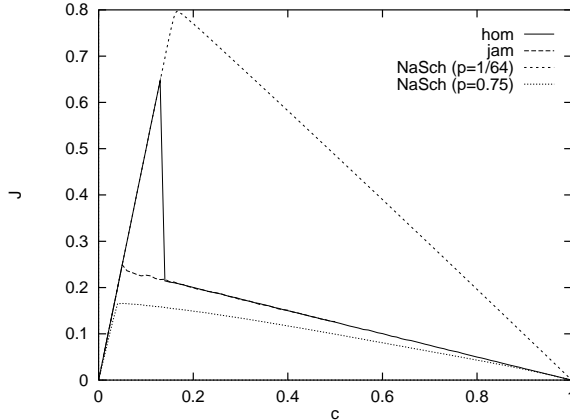


Fig. 9. The fundamental diagram in the NaSch model with a velocity-dependent slow-to-start rule ($v_{max} = 5$, $p_0 = 0.75$, $p = 1/64$) obtained using two different initial conditions, namely, a completely jammed state (jam) and a homogeneous state (hom).

ues depending on the initial state and, therefore, exhibit metastability. The microscopic structure of the states in the free-flow branch is very similar to that of the NaSch model. The metastable homogeneous states have a lifetime after which their decay leads to congested branch (see Fig. 10). In contrast, the microscopic structure of the congested branch differs drastically from the NaSch model. Here one observes phase separation into a macroscopic jam and a macroscopic free-flow regime (see Fig. 10).

It is instructive to compare the fundamental diagram of the VDR model with those of the corresponding NaSch models. The fundamental diagram of the VDR model can be understood from heuristic arguments utilizing the observed structures of the steady-states. For small densities $\rho \ll 1$ there are no slow cars in the VDR model since interactions between cars are extremely rare. Every car moves with the free-flow velocity $v_f = v_{max} - p$ and, therefore, the flux is given by

$$J_{hom}(\rho) = \rho(v_{max} - p) \quad (2)$$

which is identical to the NaSch model with randomization p . On the other hand, for densities close to $\rho = 1$, the cars are likely to have velocities $v = 0$ or $v = 1$ only and, therefore, the random braking is dominated by p_0 . A simple waiting time argument [34] shows that the flow in the phase-separated regime

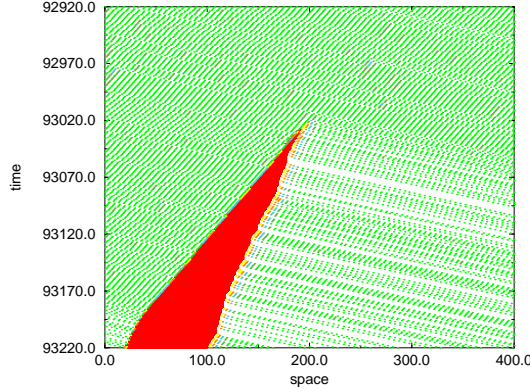


Fig. 10. Typical space-time diagram of the VDR model with $v_{max} = 5$ and $\rho = 0.20$, $p = 0.01$ and $p_0 = 0.75$. Each horizontal row of dots represents the instantaneous positions of the cars moving towards right while the successive rows of dots represent the positions of the same cars at the successive time steps.

is given by

$$J_{sep}(\rho) = (1 - p_0)(1 - \rho). \quad (3)$$

This corresponds to the NaSch model with randomization p_0 (see Fig. 9).

The behaviour found in the VDR model is generic for models with slow-to-start rules. Due to the slow-to-start rule the outflow from a large jam is smaller than the maximal possible flow, i.e. the maximum of the fundamental diagram. Therefore the density far downstream is rather small and the vehicles propagate almost freely in the low-density region. The spontaneous formation of jams is suppressed if p is not too large. This is the basic mechanism which leads to the formation of the phase-separated state and hysteresis.

4.2 Anticipation and synchronized traffic

In the NaSch model as well as in the VDR model drivers only react to the distance to the next car ahead, i.e. the headway. In real traffic often “anticipation” plays an important role. Drivers not only react to a change of their headway, but also take into account the headway of the preceding car. If this headway is large the preceding car will not brake sharply and therefore much shorter distances between cars are acceptable.

Fig. 11 gives an example for this kind of behaviour. It shows empirical data for time-headways, i.e. the time intervals between the passing of consecutive cars recorded by a detector at a fixed position on the highway. The time-headway distribution in the free-flow regime shows a two peak structure. The

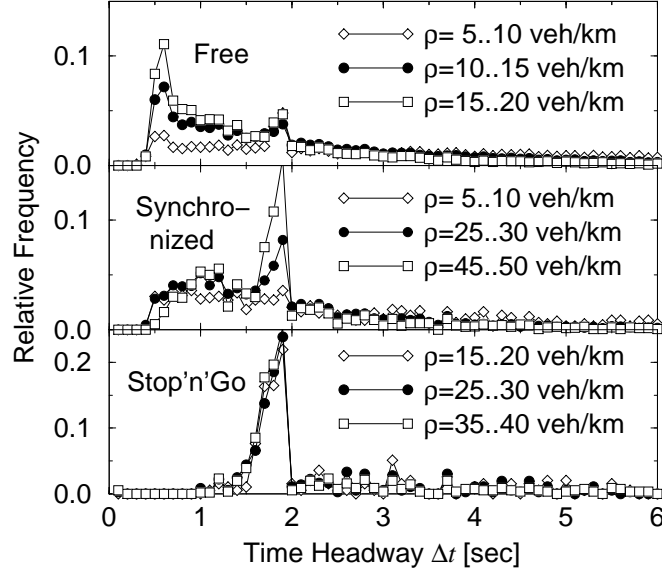


Fig. 11. Time-headway distribution for different density regimes. Top: In free-flow traffic the Δt -distribution is dominated by two peaks at 0.8sec and 1.8sec. Middle: In synchronized traffic cars with narrow time gaps are to find as well as a dominating peak. Bottom: In stop-and-go traffic short time headways are suppressed. The peak at 1.8sec remains since vehicles are leaving the jam with a typical temporal headway of approximately 2sec.

peak at $\Delta t = 1.8$ sec corresponds to the recommended safe distance⁴. What is surprising is the existence of a second even larger peak at $\Delta t = 0.8$ sec. On a microscopic level these short time-headways correspond to platoons of some vehicles traveling very fast – their drivers are taking the risk of driving "bumper-to-bumper" with a rather high speed. These platoons are the reason for the occurrence of high-flow states in free traffic. The corresponding states exhibit metastability, i.e. a perturbation of finite magnitude and duration is able to destroy such a high-flow state [23].

The NaSch model is not able to reproduce this behaviour. In [35] an extension of the NaSch model has been introduced which includes anticipation as a crucial ingredient. The driving strategy of the drivers in this model comprises four aspects:

- (i) At large distances the cars move (apart from fluctuations) with their desired velocity v_{max} .
- (ii) At intermediate distances drivers react to velocity changes of the next vehicle downstream, i.e. to "brake lights".
- (iii) At small distances the drivers adjust their velocity such that safe driving is possible.
- (iv) The acceleration is delayed for standing vehicles and directly after braking events. This is achieved by introducing an interaction horizon and brake lights. The

⁴ This corresponds to the following rule of thumb taught in (German) driving schools: safe distance (in meters) = half of velocity (in km/h).

randomization parameter obeys a slow-to-start rule and in addition depends on the state of the brake light. Furthermore a finer discretization of the lattice allows for a more realistic modelling of the acceleration behaviour.

This model is also able to reproduce the typical behaviour found in so-called synchronized traffic. As first pointed out by Kerner and Rehborn [12,22,36,37] the congested phase can be divided into stop-and-go and synchronized traffic. In the latter, the mean velocity is considerably reduced, but all cars are moving and the flow is rather large.

A statistical observable which allows to identify synchronized traffic is the crosscorrelation

$$cc_{J\rho} = \frac{1}{\sqrt{\sigma(J)\sigma(\rho)}} [\langle J(t)\rho(t+\tau) \rangle - \langle J(t) \rangle \langle \rho(t+\tau) \rangle] \quad (4)$$

($\sigma(\xi)$ denotes the variance of ξ) between the density ρ and the flow J almost vanishes [38]. This means that these variables are almost independent of each other and the data points cover randomly a plane in the fundamental diagram [12]. In contrast, in the free-flow phase the flow is completely determined by the density and $cc_{J\rho}(\tau) \approx 1$.

Another interesting property of synchronized traffic is the existence of strong velocity correlations between the lanes in multilane highways. Lane changes are strongly suppressed and the traffic in the different lanes becomes “synchronized”. For a discussion of further features of synchronized flows and transitions between the different phases we refer to [12] (and refs. therein).

5 Effects of on- and off-ramps

There is large empirical evidence that the activity of on- and off-ramps can trigger transitions from free to congested flow [38,39]. This view was supported by analysis of macroscopic models, where the introduction of on ramps leads to synchronized flow like behaviour [40,41].

In a very recent work [42], which I will summarize in the following subsection, simulations of microscopic models with different types of ramps have been discussed. In Sec. 5.2 experimental evidence [43] for the nonequilibrium phase transitions predicted by the ASEP (see Sec. 3.1) will be presented.

5.1 Ramps in periodic systems

First we discuss implementations of on- and off-ramps in single-lane systems with periodic boundary conditions where the number of cars is constant. The on- and off-ramps are implemented as connected parts of the lattice where the vehicles may enter or leave the system (see Fig. 12). The activity of the ramps is characterised by the number of entering (or leaving) cars per unit of time j_{in} (j_{out}). A car is only added to the system if the removal of another car at the off-ramp is possible at the *same* time-step so that $j_{in} = j_{out}$. In [42] input and output are performed with a constant frequency. A stochastic in- and output of cars does not lead to a qualitatively different behaviour. The length chosen for the on- and off-ramps and the distance between them is motivated by the dimensions found on german highways: $L_{ramp} = 25$ as length of the ramps in units of the lattice constant (usually identified with 7.5 meters). The position, i.e. the first cell of the on-ramp, is located at $x_{on} = 80$ and that of the off-ramp at $x_{off} = L - 80$ where L is the system size. Using periodic boundary conditions the distance of the on-ramp to the off-ramp is given by $d_{ramp} = x_{on} - x_{off} + L$.

Two different procedures for adding cars to the lattice have been investigated in order to model inconsiderate (type A) and cautious behaviour (type B) of the drivers at the ramp. The only and essential difference in the implementation of the different types of on-ramps lies in the strategy of the cars changing from the acceleration lane to the driving lane. It has been found that all the procedures give qualitatively the same results.

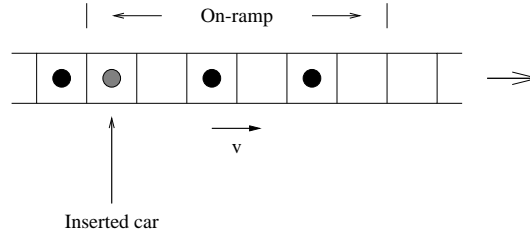


Fig. 12. Schematical representation of the on-ramp.

In Fig. 13 the fundamental diagrams of the NaSch model for both types of on-ramps are shown for the input-rate $j_{in} = j_{out} = \frac{1}{5}$. For comparison the fundamental diagram without ramps is also shown as solid line.

It is clearly seen that a density regime $\rho_{low} < \rho < \rho_{high}$ exists where the flow $J(\rho)$ is independent of the density. This so-called plateau value of the flow is lower than the corresponding flow of the model without ramps. An increase of the input-rate j_{in} leads to a decrease of the plateau value. If one compares the different types of input strategies it is evident that the plateau value of type B is lower than that of type A. This can be explained by the probability that the cell in front of the inserted car is already occupied. For type B (cautious)

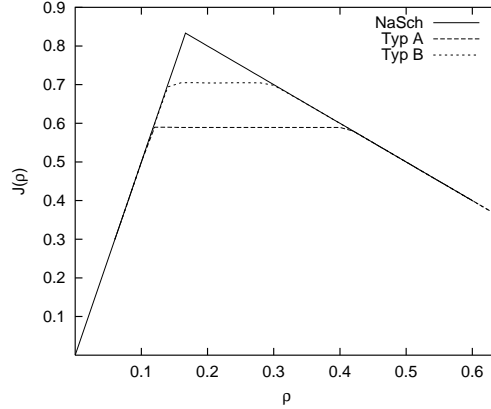


Fig. 13. Fundamental diagrams of both ramp types at the same input-rate $j_{in} = \frac{1}{5}$. The model parameters are given by $L = 3000, v_{max} = 5, p = 0$.

this probability is smaller than for type A (inconsiderate). Nevertheless there is no difference between the two types in a qualitative sense.

One can distinguish three different phases depending on the global density. In the high and low density phases the average flow $J(\rho)$ of the perturbed system takes the same value as in the system without ramps. For intermediate densities $\rho_{low} < \rho < \rho_{high}$ the flow is constant and limited by the capacity of the ramps.

This behaviour can be understood from the form of the density profiles (see Fig. 14). In the high and low density phase one only observes local deviations from a constant density profile. For intermediate densities, however, the system is separated into macroscopic high (ρ_{high}) and low (ρ_{low}) density regions. In the region of the ramps the density ρ_{ramp} is additionally higher than in the high density region. Thus the ramps act like a blockage in the system that decreases the flow locally. Varying the global density within the phase-separated state the bulk densities in the high and low density region remain constant, only the length of the regions changes. Also the local density at the ramps (ρ_{ramp}) remains constant. Finally this leads to a constant flow in the segregated phase.

This phase separation in systems with ramps and the form of the fundamental diagram is very similar to the behaviour found in systems with a stationary defect [44–46]. Typically, in a certain range on the lattice the slowdown parameter p is increased to a value $p_d > p$ compared to that of the residual lattice sites [44–46]. For intermediate densities $\rho_{low} < \rho < \rho_{high}$ the flow is constant in analogy to the model with ramps. In this regime $J(\rho)$ is limited by the capacity of the defect sites. There is no qualitative difference between the effect of on- and off-ramps and that of stationary defects. In both cases one observes plateau formation in the fundamental diagram as well as phase separation in the system. The only difference lies in the nature of the blockage dividing the system into two macroscopic regions. In the case of the ramps it

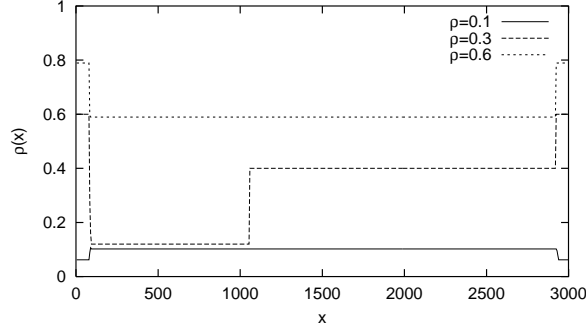


Fig. 14. Density profiles in the three phases. In the high ($\rho = 0.60$) and low ($\rho = 0.10$) density phases only local inhomogeneities occur near the ramps ($x_{on} = 80, x_{off} = L - 80$). For intermediate densities ($\rho = 0.30$) one observes phase separation. The model parameters are the same used in Fig. 13.

is the local increase of the density that decreases the flow locally. In the model with defects the increased slowdown parameter leads to a local decrease of the flow.

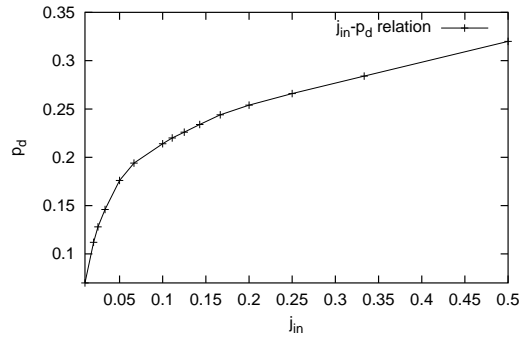


Fig. 15. Relation between the input-rates j_{in} and the slowdown parameter p_d at the defect sites.

In order to use the equivalence of ramps and defects in realistic simulations of traffic flow one has to determine the relation between the input-rates j_{in} and the slowdown parameter p_d at the defect sites. Fig. 15 shows the values of p_d and j_{in} leading to the same fundamental diagrams. It can be seen that a non-trivial relation between the two parameters exists.

This analogy is very important for efficient modelling of complex networks [13] with a multitude of ramps. Therefore it seems to be possible to achieve a considerable reduction of the computational complexity of network simulation using this kind of implementation of ramps.

5.2 Ramps in open systems

In [33] it has been shown that empirical data obtained in measurements on a German highway near Cologne can be interpreted using the results presented in Sec. 3.1. These experimental data exhibit boundary effects caused by the presence of an on-ramp. Fig. 16 shows a sketch of the relevant part of the highway. No experimental data are available for the density ρ^- and flow $j^- = j(\rho^-)$ far upstream from the on-ramp and ρ^+ and $j^+ = j(\rho^+)$ just before the on-ramp as well as the activity of the ramp. The only data come from a detector located upstream from the on-ramp which measures a traffic density $\hat{\rho}$ and the corresponding flow \hat{j} .

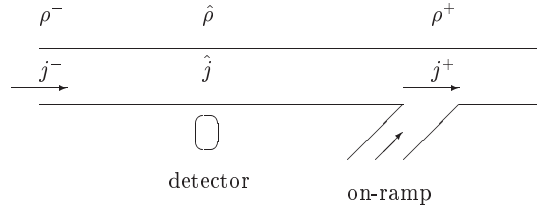


Fig. 16. Schematic road design of a highway with an on-ramp where cars enter the road. The arrows indicate the direction of the flow. The detector measures the local bulk density $\hat{\rho}$ and bulk flow \hat{j} .

Cars entering the motorway cause the mainstream of vehicles to slow down locally. Therefore, the vehicle density just before the on-ramp increases to $\rho^+ > \rho^-$. Then a shock, formed at the on-ramp, will propagate with mean velocity

$$v_{shock} = \frac{j(\rho^+) - j(\rho^-)}{\rho^+ - \rho^-}, \quad (5)$$

obtained from mass conservation. v_{shock} is the velocity of a 'domain-wall' ⁵ between two stationary regions of densities ρ^-, ρ^+ . The formation of a stable shock is usually a boundary-driven process caused by a 'bottleneck' on a road. Bottlenecks on a highway arise from a reduction in the number of lanes and from on-ramps where additional cars enter a road (see Sec. 5.1).

Depending on the sign of v_{shock} , two scenarios are now possible:

1) $v_{shock} > 0$ (i.e. $j^+ > j^-$): In this case the shock propagates (on average) downstream towards the on-ramp. Only by fluctuations a brief upstream motion is possible. Therefore the detector will measure a traffic density $\hat{\rho} = \rho^-$ and flow $\hat{j} = j^-$.

⁵ In nonequilibrium systems a domain wall is an object connecting two possible stationary states.

2) $v_{shock} < 0$ (i.e. $j^+ < j^-$): The shock wave starts propagating with the mean velocity v_{shock} upstream, thus expanding the congested traffic region with density ρ^+ . The detector will now measure $\hat{\rho} = \rho^+$ and flow $\hat{j} = j^+$.

In order to discuss the transition between these two scenarios suppose that one starts with a situation where $j^+ > j^-$ is realized. If now the far-upstream-density ρ^- increases it will reach a critical point ρ_{crit} above which $j^- > j^+$, i.e., the free flow upstream j^- prevails over the flow j^+ which the ‘bottleneck’, i.e. the on-ramp, is able to support. At this point shock wave velocity v_{shock} will change sign (see (5)) and the shock starts traveling upstream. As a result, the stationary bulk density $\hat{\rho}$ measured by the detector upstream from the on-ramp will change discontinuously from the critical value ρ_{crit} to ρ^+ . This marks a nonequilibrium phase transition of first order with respect to order parameter $\hat{\rho}$. The discontinuous change of $\hat{\rho}$ leads also an abrupt reduction of the local velocity. Notice that the flow $\hat{j} = j^+$ through the on-ramp (then also measured by the detector) will stay *independent* of the free flow upstream from the congested region j^- as long as the condition $j^- > j^+$ holds.

Empirically this phenomenon can be seen in the traffic data taken from measurements on the motorway A1 close to Cologne [38]. Fig. 17 shows a typical time series of the one-minute velocity averages. One can clearly see the sharp drop of the velocity at about 8 a.m.

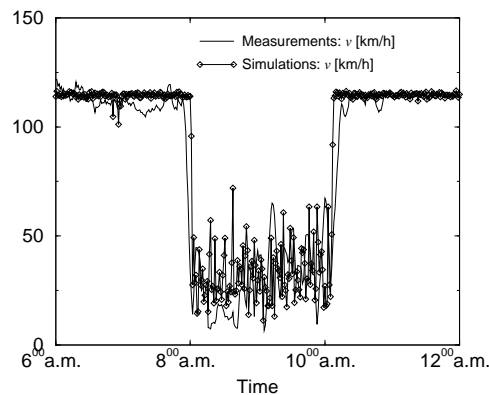


Fig. 17. Time series of the velocity. Each data point represents an one-minute average of the speed. Shown are empirical data (from [38]) in comparison with the results of computer simulations using a NaSch model with boundary reservoirs.

Also the measurements of the flow versus local density, i.e. the fundamental diagram (Fig. 18), support this interpretation. Two distinct branches can be distinguished. The increasing part corresponds to an almost linear rise of the flow with density in the free-flow regime. This part of the flow diagram is not affected by the presence of the on-ramp at all and one measures $\hat{j} = j^-$ which is the actual upstream flow. The second branch are measurements taken during congested traffic hours. The transition from free flow to congested traffic is characterized by a discontinuous reduction of the local velocity. However, as

predicted above the flow does not change significantly in the congested regime. In contrast, in local measurements large density fluctuations can be observed. Therefore in this regime the density does not take the constant value ρ^+ as suggested by the argument given above, but varies from 20 veh/km/lane to 80 veh/km/lane (see Fig. 18). In contrast, spontaneously emerging and decaying jams would lead to the observation of a non-constant flow.

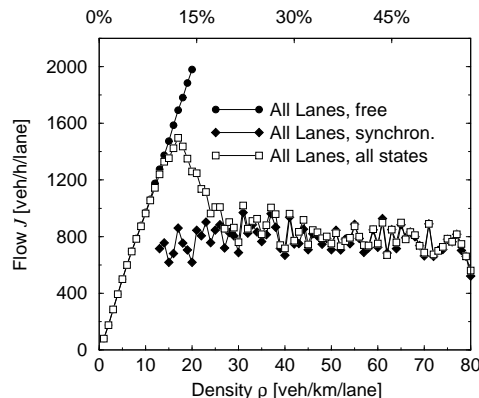


Fig. 18. Measurements of the flow versus local density before an on-ramp on the motorway A1 close to Cologne. The detector is located at a distance 1 km upstream from on-ramp.

This shows that the empirical data obtained near an on-ramp can indeed be interpreted as a nonequilibrium phase transition. Furthermore it shows exactly the same behaviour as the transition from the low-density to the high-density phase in the ASEP (see Sec. 3.1).

The case of an off-ramp (or expansion of road space etc.) leads to a local decrease $\rho^+ < \rho^-$ of the density. Here the collective velocity $v_c = \frac{\partial j(\rho)}{\partial \rho}$ plays an important role. The theory then predicts a transition from the free-flow regime to the maximal flow (MF) phase [43]. This transition is of second order because $\hat{\rho}$ changes continuously across the phase transition point and has not yet been observed empirically. The existence of a maximal flow phase was not emphasized in the context of traffic flow up to now. At the same time, it is the most desirable phase, carrying the maximal possible throughput of vehicles j_{max} .

For practical purposes above observations may directly be used in order to operate a highway in the optimal regime. E.g. the flow near a lane reduction could be increased significantly if the traffic state at the entry would allow to attain the maximal possible flow of the bottleneck. This could be achieved by controlling the density far upstream, e.g. by closing temporally an on-ramp, such that the cars still enter the bottleneck with high velocity.

6 Summary and conclusion

In this short review only a few examples for the successful application of CA models for the description of traffic flow have been presented. Despite its conceptual simplicity the NaSch model and its variants are able to reproduce many phenomena observed empirically. Although the same is true for many of the other approaches mentioned here only briefly in the introduction CA have the big advantage of being ideally suited for large-scale computer simulations. It is now possible to simulate large networks of highway [47] and city traffic [48–50] faster than real time. This offers new perspectives for the planning and design of transportation networks. Finally it is worthwhile pointing out that not only traffic science profits from the application of methods from physics. The example of the first empirical observation of a boundary-induced phase transition (see Sec. 5.2) shows that also physics can profit from applications to "exotic fields".

Acknowledgements: I like to thank all my collaborators, especially L. Santen and D. Chowdhury for their contribution to the extensive review [1]. I also like to thank the organizers of the 36. Karpacz Winter School for creating a stimulating atmosphere.

References

- [1] D. Chowdhury, L. Santen, A. Schadschneider, Phys. Rep. **329**, 199 (2000) and Curr. Sci. **77**, 411 (1999)
- [2] R. Herman and K. Gardels, Sci. Am. **209**(6), 35 (1963)
- [3] L.A. Pipes, J. Appl. Phys. **24**, 274 (1953)
- [4] M. Bando, K. Hasebe, A. Nakayama, A. Shibata and Y. Sugiyama, Phys. Rev. E **51**, 1035 (1995); Jpn. J. Ind. Appl. Math. **11**, 202 (1994)
- [5] M.J. Lighthill and G.B. Whitham, Proc. Roy. Soc. Lond. A **229**, 281 (1955)
- [6] I. Prigogine and R. Herman, *Kinetic Theory of Vehicular Traffic* (Elsevier, Amsterdam, 1971)
- [7] D.E. Wolf, M. Schreckenberg and A. Bachem (eds.), *Traffic and Granular Flow* (World Scientific, Singapore, 1996)
- [8] M. Schreckenberg and D.E. Wolf (eds.), *Traffic and Granular Flow '97* (Springer, Singapore, 1998)
- [9] A.D. May, *Traffic Flow Fundamentals* (Prentice-Hall, 1990)
- [10] D. Helbing, *Verkehrsdynamik: Neue Physikalische Modellierungskonzepte* (in German) (Springer, 1997)
- [11] D.E. Wolf, Physica A **263**, 438 (1999)
- [12] B.S. Kerner, Phys. World **8**, 25 (1999)
- [13] K. Nagel, J. Esser and M. Rickert, in: Annu. Rev. Comp. Phys. **7**, p. 151, ed. D. Stauffer (World Scientific, 2000)
- [14] B. Schmittmann and R.K.P. Zia, in: *Phase Transitions and Critical Phenomena*, Vol. 17, eds. C. Domb and J.L. Lebowitz (Academic Press, 1995)
- [15] V. Privman (ed.), *Nonequilibrium Statistical Mechanics in One Dimension* (Cambridge University Press, 1997)
- [16] J. Marro and R. Dickman, *Nonequilibrium Phase Transitions in Lattice Models* (Cambridge University Press, 1999)
- [17] G.M. Schütz, in: *Phase Transitions and Critical Phenomena*, Vol. 19, eds. C. Domb and J.L. Lebowitz (Academic Press, 2000)
- [18] S. Wolfram, *Theory and Applications of Cellular Automata*, (World Scientific, 1986); *Cellular Automata and Complexity* (Addison-Wesley, 1994)
- [19] B. Chopard and M. Droz, *Cellular Automata Modelling of Physical Systems* (Cambridge University Press, 1998)
- [20] J. Treiterer: Ohio State Technical Report No. PB 246 094, (1975)

- [21] B.S. Kerner and H. Rehborn, Phys. Rev. E **53**, R1297 (1996)
- [22] B.S. Kerner and H. Rehborn, Phys. Rev. E **53**, R4275 (1996)
- [23] B.S. Kerner, in [8], p. 239
- [24] F.L. Hall, B.L. Allen and M.A. Gunter, Transp. Res. **A20**, 197 (1986)
- [25] K. Nagel and M. Schreckenberg, J. Physique I, **2**, 2221 (1992)
- [26] M. Schreckenberg, A. Schadschneider, K. Nagel and N. Ito, Phys. Rev. E **51**, 2939 (1995)
- [27] G. Schütz and E. Domany, J. Stat. Phys. **72**, 277 (1993)
- [28] B. Derrida, M.R. Evans, V. Hakim and V. Pasquier, J. Phys. A **26**, 1493 (1993)
- [29] N. Rajewsky, L. Santen, A. Schadschneider and M. Schreckenberg, J. Stat. Phys. **92**, 151 (1998)
- [30] M.R. Evans, N. Rajewsky and E.R. Speer, J. Stat. Phys. **95**, 45 (1999)
- [31] J. de Gier and B. Nienhuis, Phys. Rev. E **59**, 4899 (1999)
- [32] A.B. Kolomeisky, G. Schütz, E.B. Kolomeisky and J.P. Straley, J. Phys. A **31**, 6911 (1998)
- [33] V. Popkov and G. Schütz, Europhys. Lett. **48**, 257 (1999)
- [34] R. Barlovic, L. Santen, A. Schadschneider and M. Schreckenberg, Eur. Phys. J. B **5**, 793 (1998)
- [35] W. Knospe, L. Santen, A. Schadschneider and M. Schreckenberg, preprint (2000)
- [36] B.S. Kerner and H. Rehborn, Phys. Rev. Lett. **79**, 4030 (1998)
- [37] B.S. Kerner, Phys. Rev. Lett. **81**, 3797 (1998)
- [38] L. Neubert, L. Santen, A. Schadschneider and M. Schreckenberg, Phys. Rev. E **60**, 6480 (1999)
- [39] C.F. Daganzo, M.J. Cassidy, R.L. Bertini, Transp. Res. A **33**, 365 (1999)
- [40] H.Y. Lee, H.-W. Lee, D. Kim, Phys. Rev. Lett. **81**, 1130 (1998); Phys. Rev. E **59**, 5101 (1999)
- [41] D. Helbing, M. Treiber, Phys. Rev. Lett. **81**, 3042 (1998)
- [42] G. Diedrich, L. Santen, A. Schadschneider and J. Zittartz, Int. J. Mod. Phys. **C11**, 335 (2000)
- [43] V. Popkov, L. Santen, A. Schadschneider and G.M. Schütz, `cond-mat/0002169`
- [44] S.A. Janowsky and J.L. Lebowitz, Phys. Rev. A **45**, 618 (1992); J. Stat. Phys. **77**, 35 (1994)

- [45] W. Knospe, L. Santen, A. Schadschneider, M. Schreckenberg, in [8], p. 349 (and refs. therein)
- [46] L. Santen, *Numerical Investigations of Discrete Models for Traffic Flow*, Ph.D. thesis, Universität zu Köln (1999)
- [47] M. Rickert, Diploma thesis, Universität zu Köln (1994); K. Nagel, Ph.D. thesis, Universität zu Köln (1995)
- [48] J. Esser and M. Schreckenberg, Int. J. Mod. Phys.C **8**, 1025 (1997).
- [49] M. Rickert and K. Nagel, Int. J. Mod. Phys.C **8**, 483 (1997); K. Nagel and C.L. Barrett, Int. J. Mod. Phys. C **8**, 505 (1997)
- [50] B. Chopard, A. Dupuis and P. Luthi, in ref. [8], p. 153